International Journal of Applied Engineering Research ISSN 0973-4562 Volume 14, Number 16 (2019) pp. 3541-3551

Effects of Hall and Heat Transfer on the Peristaltic Transport of a Conducting Newtonian Fluid through Porous Medium in a Vertical Asymmetric Channel

[1]RudraRaviKumar Palegari [2]Dr.R.SivaPrasad

Department of Mathematics, RGUKT-APIIIT, Idupulapaya, Kadapa District, A.P., India.

Abstract

The effects of heat transfer and Hall on the peristaltic flow of a Newtonian fluid through a porous medium in an asymmetric vertical channel, by using Lubrication approach. The expressions for velocity and pressure rise are obtained. The effects of free convection parameter Gr, heat source/sink parameter β, Hartmann number M, Darcy number Da, Hall parameter m, phase shift φ, amplitude of the upper wave ϕ_1 and lower wave ϕ_2 on the pumping characteristics and the heat transfer coefficient are evaluated numerically

Keywords: Hall Effect, Vertical Asymmetric Channel, Porous Medium, Heat Transfer, Peristaltic flow

1. INTRODUCTION

Quite a few of the physiological systems in human body cannot be modeled by a symmetrical channel, mainly the sagittal cross section of the uterus. Eytan and Elad [5] and Eytan et al. [6] have studied the intra uterine fluid in the sagittal cross section of the uterus by an asymmetric channel under long wavelength approximation. Mishra and Ramachandra Rao [10 have studied the flow of Newtonian fluid in an asymmetric channel generated by peristaltic waves propagating on the walls. Mishra and Ramachandra Rao [10] obtained a perturbation solution for the problem of peristaltic flow of a viscous Newtonian fluid in an asymmetric channel. Nagendra et al. [11] have studied the peristaltic flow of a power- law fluid in an asymmetric vertical channel.

Hall effect plays an important role, in particular when the Hall parameter is very high. This occurs when either the density of an electrically conducting fluid is low and/or the applied magnetic field is strong. Customarily, the Hall term is ignored in Ohm's law, as it has no manifest character for small and adequate values of the magnetic field. Nevertheless, the current tendency with a strong magnetic field is always noticeable and has a great influence on the electromagnetic force. Under these circumstances, the Hall current has an abundant impact and noticeable effects on the magnitude, direction of the current density, and eventually on the magnetic-force term. Therefore, it is of great interest to study the influence of the Hall current on the flow, as the Hall current determines the flow features of the problem. Hayat et al. [8] have first investigated the Hall effects on the peristaltic flow of a Maxwell fluid trough a porous medium in channel. Eldabe [4] have studied the Hall Effect on peristaltic flow of third order fluid in a porous medium with heat and mass transfer. Effect of hall and ion slip on peristaltic blood flow of Eyring Powell fluid in a non-uniform porous channel was studied by Bhatti et al. [1]. Moreover, flow through a porous medium has been studied by a number of researchers employing Darcy's law Scheidegger [12]. The first study of peristaltic flow through a porous medium is presented by Elsehawey et al. [2]. Elsehawey et al. [3] investigated the peristaltic motion of a generalized Newtonian fluid through a porous medium. Non-linear peristaltic transport through a porous medium in an inclined planar channel has studied by Mekheimer [9] taking the gravity effect on pumping characteristics.

Understanding of bio-heat transport is an important in the advantageous applications of heat and cold for medical treatment. Recent advances in the application of heat (hyperthermia), radiation (laser therapy), and coldness (cryosurgery), as means to destroy undesirable tissues, such as cancer, have stimulated much interest in the study of thermal modeling in tissue. Srinivas and Kothandapani [13] have discussed the influence of MHD and heat transfer on the peristaltic flow of a Newtonian in an asymmetric channel. Effect of heat transfer on peristaltic transport of a Newtonian fluid through a porous medium in an asymmetric vertical channel was investigated by Vasudev et al. [14]. Govindarajan et al. [7] have studied the combined effect of heat and mass transfer on MHD peristaltic transport of a couple stress fluid in a inclined asymmetric channel through a porous medium

In view of these, we study the effects of heat transfer and Hall on the peristaltic flow of a Newtonian fluid through a porous medium in an asymmetric vertical channel, by using Lubrication approach. The expressions for velocity and pressure rise are obtained. The effects of free convection parameter Gr, heat source/sink parameter β, Hartmann number M, Darcy number Da, Hall parameter m, phase shift φ, amplitude of the upper wave ϕ_1 and lower wave ϕ_2 on the pumping characteristics and the heat transfer coefficient are evaluated numerically and discussed in detail with the help of graphs.

2. MATHEMATICAL FORMULATION

We consider the peristaltic transport of a viscous incompressible conducting fluid through a porous medium in

a vertical channel with flexible walls with asymmetry being generated by the propagation of waves on the channel walls traveling with same speed c but with different amplitudes and phases. The lower and upper walls of the channel are maintained at constant temperatures T_1 and T_0, respectively. Fig.1. shows the physical model of the asymmetric channel.

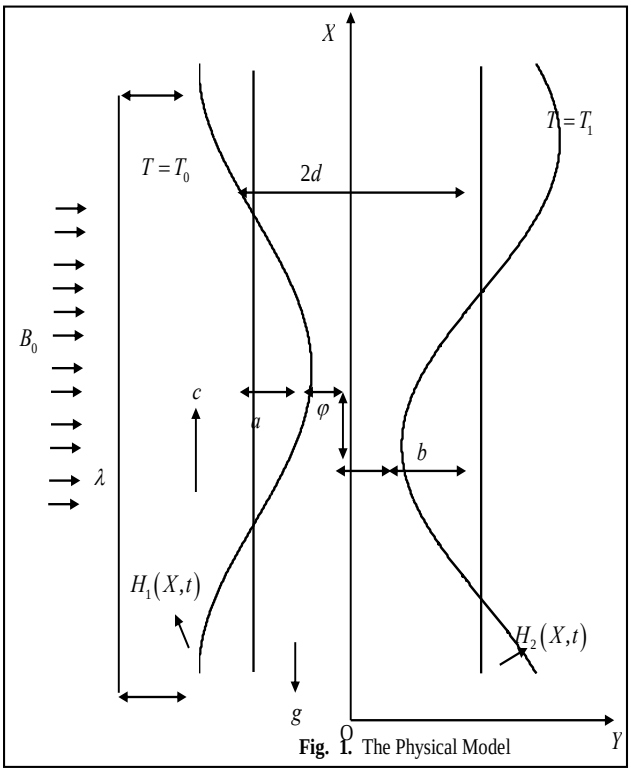

Fig. 1. The Physical Model

The channel walls are given by

$$Y = H_1(X,t) = d + a\cos\frac{2\pi}{\lambda}(X - ct)$$

(upper wall) (2.1a)

$$Y = H_2(X,t) = -d - b\cos\left(\frac{2\pi}{\lambda}(X - ct) + \varphi\right)$$

(lower wall) (2.1b)

where a, b are the amplitudes of the waves, λ is the wavelength, $2d$ is the width of the channel, φ is the phase difference $(0 \le \varphi \le \pi)$ and t is the time.

We introduce a wave frame of reference $(x,\ y)$ moving with velocity c in which the motion becomes independent of time when the channel length is an integral multiple of the wavelength and the pressure difference at the ends of the channel is a constant. The transformation from the fixed frame of reference $(X,\ Y)$ to the wave frame of reference $(x,\ y)$ is given by

$x = X - c\ t,\ y = Y,\ \ u = U - c,\ \ v = V$ and $p(x) = P(X,\ t),$

where $(u,\ v)$ and $(U,\ V)$ are the velocity components, p and P are pressures in the wave and fixed frames of reference, respectively.

The equations governing the flow in wave frame of reference are given by

$$\frac{\partial u}{\partial x} + \frac{\partial v}{\partial y} = 0, \tag{2.2}$$

$$\rho\left(u\frac{\partial u}{\partial x} + v\frac{\partial u}{\partial y}\right) = \begin{pmatrix} -\dfrac{\partial p}{\partial x} + \mu\left(\dfrac{\partial^2 u}{\partial x^2} + \dfrac{\partial^2 u}{\partial y^2}\right) + \dfrac{\sigma B_0^2}{1+m^2}\left(mv - (u+c)\right) \\ -\dfrac{\mu}{k}(u+c) + \rho g\alpha\left(T - T_0\right) \end{pmatrix} \tag{2.3}$$

$$\rho\left(u\frac{\partial v}{\partial x} + v\frac{\partial v}{\partial y}\right) = -\frac{\partial p}{\partial y} + \mu\left(\frac{\partial^2 v}{\partial x^2} + \frac{\partial^2 v}{\partial y^2}\right) - \frac{\sigma B_0^2}{1+m^2}\left(m(u+c) + v\right) - \frac{\mu}{k}v \tag{2.4}$$

$$\rho c_p\left(u\frac{\partial T}{\partial x} + v\frac{\partial T}{\partial y}\right) = k\left(\frac{\partial^2 T}{\partial x^2} + \frac{\partial^2 T}{\partial y^2}\right) + Q_0 \tag{2.5}$$

where k_0 is the permeability of the porous medium, ρ is the density, T is the temperature, α is the coefficient of linear thermal expansion of the fluid, g is the acceleration due to gravity, k is thermal conductivity, c_p is the specific heat at constant pressure, Q_0 is the constant heat addition/absorption, μ is the viscosity of the fluid.

Introducing the following non-dimensional variables

$$\bar{x}=\frac{x}{\lambda},\bar{y}=\frac{y}{d},\bar{u}=\frac{u}{c},\bar{v}=\frac{v}{c\delta},\delta=\frac{d}{\lambda},\bar{p}=\frac{pd^2}{\mu c\lambda},\beta=\frac{d^2Q_0}{k\left(T_1-T_0\right)}$$

$$\theta=\frac{T-T_0}{T_1-T_0},h_1=\frac{H_1}{d},h_2=\frac{H_2}{d},\phi_1=\frac{a}{d},\phi_2=\frac{b}{d},Gr=\frac{\rho g\alpha d^2\left(T_1-T_0\right)}{c\mu}$$

in the governing equations (2.1)-(2.5), and dropping the bars, we get

$$h_1=1+\phi_1\cos 2\pi x,\ h_2=-1-\phi_2\cos\left(2\pi x+\varphi\right) \tag{2.6}$$

$$\frac{\partial u}{\partial x}+\frac{\partial v}{\partial y}=0 \tag{2.7}$$

$$\mathrm{Re}\,\delta\left(u\frac{\partial u}{\partial x}+v\frac{\partial u}{\partial y}\right)=\begin{pmatrix}-\dfrac{\partial p}{\partial x}+\left(\delta^2\dfrac{\partial^2 u}{\partial x^2}+\dfrac{\partial^2 u}{\partial y^2}\right)+\dfrac{M^2}{1+m^2}\left(m\delta v-\left(u+1\right)\right)\\ -\dfrac{1}{Da}\left(u+1\right)+Gr\theta\end{pmatrix} \tag{2.8}$$

$$\mathrm{Re}\,\delta^3\left(u\frac{\partial v}{\partial x}+v\frac{\partial v}{\partial y}\right)=-\frac{\partial p}{\partial y}+\delta^2\left(\delta^2\frac{\partial^2 v}{\partial x^2}+\frac{\partial^2 v}{\partial y^2}\right)-\frac{\delta M^2}{1+m^2}\left(m\left(u+1\right)+\delta v\right)-\frac{\delta^2}{Da}v \tag{2.9}$$

$$\mathrm{Re}\,\mathrm{Pr}\,\delta\left(u\frac{\partial \theta}{\partial x}+v\frac{\partial \theta}{\partial y}\right)=\left(\delta^2\frac{\partial^2\theta}{\partial x^2}+\frac{\partial^2\theta}{\partial y^2}\right)+\beta \tag{2.10}$$

where $\mathrm{Re}=\dfrac{\rho dc}{\mu}$ is the Reynolds number, $\mathrm{Pr}=\dfrac{\mu c_p}{k}$ is the Prandtl number, β is the dimensionless heat source/sink parameter, $Da=\dfrac{k}{d^2}$ is the Darcy number and $M=dB_0\sqrt{\dfrac{\sigma}{\mu}}$ is the Hartmann number .

Using long wavelength (i.e., $\delta<<1$) and negligible inertia (i.e., $\mathrm{Re}\to 0$) approximations, we have

$$\frac{\partial^2 u}{\partial y^2}-N^2u+Gr\theta=\frac{\partial p}{\partial x}+N^2 \tag{2.11}$$

$$\frac{\partial p}{\partial y}=0 \tag{2.12}$$

$$\frac{\partial^2\theta}{\partial y^2}+\beta=0 \tag{2.13}$$

where $N=\sqrt{\dfrac{M^2}{1+m^2}+\dfrac{1}{Da}}$.

From Eq. (2.12), it is clear that p is independent of y. Therefore Eq. (2.11) can be rewritten as

$$\frac{\partial^2 u}{\partial y^2} - N^2 u + Gr\theta = \frac{dp}{dx} + N^2 \tag{2.14}$$

The corresponding non-dimensional boundary conditions are given as

$$u = -1 \quad \text{at} \quad y = h_1 \text{ and } y = h_2 \tag{2.15}$$

$$\theta = 0 \quad \text{at} \quad y = h_1 \tag{2.16}$$

$$\theta = 1 \quad \text{at} \quad y = h_2 \tag{2.17}$$

where $h_1 = 1 + \phi_1 \cos(2\pi x)$ and $h_2 = -1 - \phi_2 \cos(2\pi x + \varphi)$.

Knowing the velocity, the volume flow rate q in a wave frame of reference is given by

$$q = \int_{h_2}^{h_1} u dy . \tag{2.18}$$

The instantaneous flow Q(X,t) in the laboratory frame is

$$Q(X,t) = \int_{h_2}^{h_1} U dY = \int_{h_2}^{h_1} (u+1) dy = q + h_1 - h_2 \tag{2.19}$$

The time averaged volume flow rate $\overline{Q}$ over one period $T\left(=\frac{\lambda}{c}\right)$ of the peristaltic wave is given by

$$\overline{Q} = \frac{1}{T}\int_0^T Q dt = q + 2 \tag{2.20}$$

3. SOLUTION

Solving Eq. (2.13) using the boundary conditions (2.16) and (2.17), we obtain

$$\theta = -\beta \frac{y^2}{2} + c_1 y + c_2 \tag{3.1}$$

where $c_1 = \dfrac{1 + \dfrac{\beta}{2}\left(h_2^2 - h_1^2\right)}{h_2 - h_1}$ and $c_2 = \beta \dfrac{h_1^2}{2} - c_1 h_1$.

Substituting Equation (3.1) in the Eq. (2.14) and solving the Eq. (2.14) using the boundary conditions (2.15), we obtain

$$u = \frac{1}{N^2}\frac{dp}{dx}\left\{c_3 \cosh(Ny) + c_4 \sinh(Ny) - 1\right\} - 1$$

$$+Gr\left\{\begin{array}{l} d_3 \cosh(Ny) + d_4 \sinh(Ny) \\ -\dfrac{\beta}{2N^2} y^2 + \left(\dfrac{c_1}{N^2}\right) y + \dfrac{1}{N^2}\left(c_2 - \dfrac{\beta}{N^2}\right) \end{array}\right\} \tag{3.2}$$

where

$$c_3 = \frac{\sinh(Nh_2) - \sinh(Nh_1)}{\sinh\left(N(h_2 - h_1)\right)}, \qquad c_4 = \frac{\cosh(Nh_1) - \cosh(Nh_2)}{\sinh\left(N(h_2 - h_1)\right)},$$

$$d_1 = \frac{\beta}{2N^2}\left[h_1^2 + \frac{2}{N^2}\right] - \frac{c_1 h_1}{N^2} - \frac{c_2}{N^2}, \quad d_2 = \frac{\beta}{2N^2}\left[h_2^2 + \frac{2}{N^2}\right] - \frac{c_1 h_2}{N^2} - \frac{c_2}{N^2},$$

$$d_3 = \frac{d_1 \sinh(Nh_2) - d_2 \sinh(Nh_1)}{\sinh\left(N(h_2 - h_1)\right)} \text{ and } d_4 = \frac{d_2 \cosh(Nh_1) - d_1 \cosh(Nh_2)}{\sinh\left(N(h_2 - h_1)\right)}.$$

The volume flow rate q is given by

$$q = \frac{1}{N^3}\frac{dp}{dx}\left[\frac{2 - 2\cosh\left(N(h_1 - h_2)\right) + N(h_1 - h_2)\sinh\left(N(h_1 - h_2)\right)}{\sinh\left(N(h_2 - h_1)\right)}\right] + Grd_5 - (h_1 - h_2) \tag{3.3}$$

where

$$d_5 = \frac{d_3}{N}\left[\sinh(Nh_1) - \sinh(Nh_2)\right] + \frac{d_4}{N}\left[\cosh(Nh_1) - \cosh(Nh_2)\right]$$
$$- \frac{\beta}{6N^2}\left(h_1^3 - h_2^3\right) + \frac{c_1}{2N^2}\left(h_1^2 - h_2^2\right) - \frac{1}{N^2}\left(\frac{\beta}{N^2} - c_2\right)(h_1 - h_2).$$

From Eq. (3.3), we have

$$\frac{dp}{dx} = \frac{N^3\left[q + h_1 - h_2 - Grd_5\right]\sinh\left(N(h_2 - h_1)\right)}{\left[2 - 2\cosh\left(N(h_1 - h_2)\right) + N(h_1 - h_2)\sinh\left(N(h_1 - h_2)\right)\right]} \tag{3.4}$$

The dimensionless pressure rise per one wavelength in the wave frame are defined as

$$\Delta p = \int_0^1 \frac{dp}{dx} dx \tag{3.5}$$

The heat transfer coefficient at the upper wall is defined by

$$Z = \frac{\partial \theta}{\partial y}\frac{\partial h_1}{\partial x}\bigg|_{y=h_1} = 2\phi_1 \pi(\beta y - c_1)\sin(2\pi x) \tag{3.6}$$

As $m \to 0$, our results coincides with the results the results of ***Vasudev et al.*** [14].

4. DISCUSSION OF THE RESULTS

In order to see the quantitative effects of the various emerging parameters involved in the results on the pumping characteristics and the heat transfer coefficient we use the MATLAB package.

Fig. 2 illustrates the variation of axial pressure gradient $\frac{dp}{dx}$ with Hartmann number M for $\phi_1 = 0.5,\ \phi_2 = 0.5,\ Gr = 1,\ m = 0.3, Da = 0.1, \beta = 1$ and $\varphi = \pi/3$. It is found that, the axial pressure gradient $\frac{dp}{dx}$ increases on increasing Hartmann number M.

The variation of axial pressure gradient $\frac{dp}{dx}$ with Hall parameter m for $\phi_1 = 0.5,\ Gr = 1,\ \phi_2 = 0.5,\ M = 1, Da = 0.1, \beta = 1$ and $\varphi = \pi/3$ is illustrated in Fig. 3. It is found that, the axial pressure gradient $\frac{dp}{dx}$ decreases with Hall parameter m.

Fig. 4 depicts the variation of axial pressure gradient $\frac{dp}{dx}$ with Darcy number Da for $\phi_1 = 0.5, \phi_2 = 0.5,\ Gr = 1,\ m = 0.3, M = 1, \beta = 1$ and $\varphi = \pi/3$. It is found that,

an increase in the Darcy number increases the axial pressure gradient $\frac{dp}{dx}$.

The variation of axial pressure gradient $\frac{dp}{dx}$ with phase shift φ for $\phi_1 = 0.5, \phi_2 = 0.5,\ Gr = 1,$ $m = 0.3, Da = 0.1, \beta = 1$ and $M = 1$ is depicted in Fig. 5. It is found that, on increasing the phase shift decreases the axial pressure gradient $\frac{dp}{dx}$.

Fig. 6 shows the variation of axial pressure gradient $\frac{dp}{dx}$ with Grashof number Gr for $\phi_1 = 0.5, \phi_2 = 0.5,\ M = 1,$ $m = 0.3, Da = 0.1, \beta = 1$ and $\varphi = \pi / 3$. It is found that, the axial pressure gradient $\frac{dp}{dx}$ increases with increasing Grashof number Gr.

The variation of axial pressure gradient $\frac{dp}{dx}$ with β for $\phi_1 = 0.5, \phi_2 = 0.5,\ Gr = 1,$ $m = 0.3, Da = 0.1, M = 1$ and $\varphi = \pi / 3$ is shown in Fig. 7. It is noted that, the axial pressure gradient $\frac{dp}{dx}$ increases with increasing sink/source parameter β.

Fig. 8 illustrates the variation of axial pressure gradient $\frac{dp}{dx}$ with ϕ_1 and ϕ_2 for $\beta = 1,\ Gr = 1,$ $m = 0.3, Da = 0.1, M = 1$ and $\varphi = \pi / 3$. It is found that, the axial pressure gradient $\frac{dp}{dx}$ increases with increasing amplitudes of the upper and lower waves of the channel.

The variation of pressure rise Δp with the time-averaged flux $\overline{Q}$ for different values of M with $\phi_1 = 0.5, \phi_2 = 0.5,\ Gr = 1,$ $m = 0.3, Da = 0.1, \beta = 1$ and $\varphi = \pi / 3$ is shown in Fig. 9. It is observed that, the time-averaged flow rate $\overline{Q}$ increases in the pumping region $(\Delta p > 0)$ with increasing M, while it decreases in both the free-pumping $(\Delta p = 0)$ and co-pumping $(\Delta p < 0)$ regions with increasing M.

Fig. 10 depicts the variation of pressure rise Δp with the time – averaged flux $\overline{Q}$ for different values of m with $\phi_1 = 0.5, \phi_2 = 0.5,\ Gr = 1,\quad M = 1, Da = 0.1, \beta = 1$ and $\varphi = \pi / 3$. It is observed that, the time-averaged flow rate $\overline{Q}$ decreases in the pumping region with an increase in m, while it increases in both the free-pumping and co-pumping regions with increasing m.

The variation of pressure rise Δp with the time – averaged flux $\overline{Q}$ for different values of Da with $\phi_1 = 0.5, \phi_2 = 0.5,\ Gr = 1,\quad m = 0.3, M = 1, \beta = 1$ and $\varphi = \pi / 3$ is depicted in Fig. 11. It is observed that, the time-averaged flow rate $\overline{Q}$ decreases in the pumping region with an increase in Da, while it increases in both the free-pumping and co-pumping regions with increasing Da.

Fig. 12 illustrates the variation of pressure rise Δp with the time – averaged flux $\overline{Q}$ for different values of θ with $\phi_1 = 0.5, \phi_2 = 0.5,\ Gr = 1,$ $m = 0.3, Da = 0.1, \beta = 1$ and $M = 1$. It is observed that, the time-averaged flow rate $\overline{Q}$ decreases in both the pumping region and free-pumping region with an increase in φ, while it increases in the co-pumping region with increasing φ for chosen $\Delta p (< 0)$.

The variation of pressure rise Δp with the time – averaged flux $\overline{Q}$ for different values of Gr with $\phi_1 = 0.5, \phi_2 = 0.5,\ M = 1,\ m = 0.3, Da = 0.1, \beta = 1$ and $\varphi = \pi / 3$ is illustrated in Fig. 13. It is observed that, the time-averaged flow rate $\overline{Q}$ increases in the pumping, free-pumping and co-pumping regions with increasing Gr.

Fig. 14 shows the variation of pressure rise Δp with the time –averaged flux $\overline{Q}$ for different values of β with $\phi_1 = 0.5, \phi_2 = 0.5,\ Gr = 1,$ $m = 0.3, Da = 0.1, M = 1$ and $\varphi = \pi / 3$. It is found that, the time-averaged flow rate $\overline{Q}$ increases in the pumping, free-pumping and co-pumping regions with increasing β.

The variation of pressure rise Δp with the time-averaged flux $\overline{Q}$ for different values of ϕ_1 and ϕ_2 with $M = 1\ Gr = 1,$ $m = 0.3, Da = 0.1, \beta = 1$ and $\varphi = \pi / 3$ is shown in

Fig. 15. It is observed that, the time-averaged flow rate $\overline{Q}$ increases in both the pumping region and free-pumping region with increasing ϕ_1 or ϕ_2, while it increases in the co-pumping region with increasing ϕ_1 or ϕ_2 for chosen $\Delta p(<0)$.

Fig. 16 shows the variation of temperature θ with phase shift φ for $\phi_1 = 0.5$, $\phi_2 = 0.5$ and $\beta = 1$. It is noted that, the temperature decreases with increasing phaseshift φ.

The variation of temperature θ with β for $\phi_1 = 0.5$, $\phi_2 = 0.5$ and $\phi = \frac{\pi}{3}$ is shown in Fig. 17. It is noted that, the temperature θ increases with increasing β.

Fig. 18 depicts the variation of temperature θ with ϕ_1 for $\varphi = \frac{\pi}{3}$, $\phi_2 = 0.5$ and $\beta = 1$. It is noted that, the temperature θ increases with increasing phseshift ϕ_1.

The variation of temperature θ with ϕ_2 for $\phi_1 = 0.5$, $\varphi = \frac{\pi}{3}$ and $\beta = 1$ is shown in Fig. 19. It is observed that, the temperature θ decreases with increasing ϕ_2.

In order to see the effects of β, φ, ϕ_1 and ϕ_2 on the heat transfer coefficient Z at the upper wall we have compute numerically and are presented in Table 1. Table 1 shows that, the heat transfer coefficient Z increases with increasing β or ϕ_1, while it decreases with increasing φ or ϕ_2.

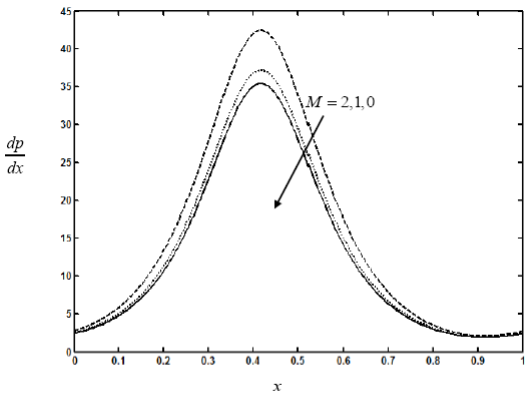

Fig. 2. The variation of axial pressure gradient $\frac{dp}{dx}$ with Hartmann number M for $\phi_1 = 0.5, \phi_2 = 0.5$, $Gr = 1$, $m = 0.3, Da = 0.1, \beta = 1$ and $\varphi = \pi/3$.

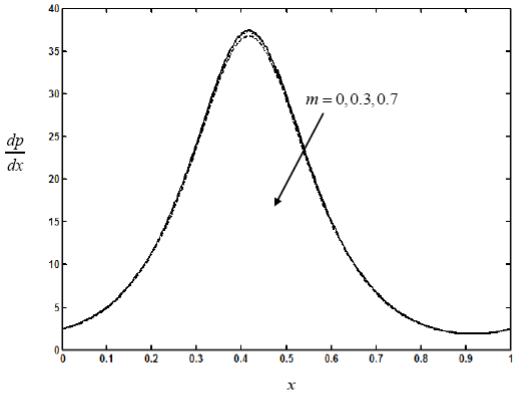

Fig. 3. The variation of axial pressure gradient $\frac{dp}{dx}$ with Hall parameter m for $\phi_1 = 0.5, \phi_2 = 0.5$, $Gr = 1$, $M = 1, Da = 0.1, \beta = 1$ and $\varphi = \pi/3$.

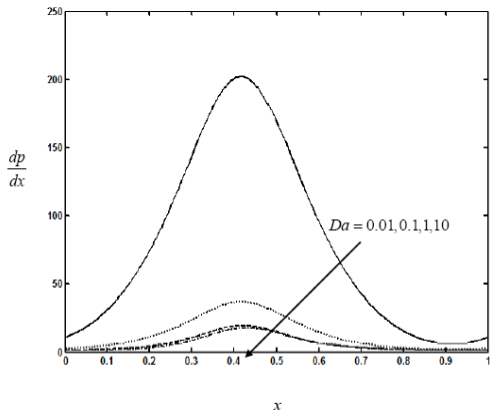

Fig. 4. The variation of axial pressure gradient $\frac{dp}{dx}$ with Darcy number Da for $\phi_1 = 0.5, \phi_2 = 0.5$, $Gr = 1$, $m = 0.3, M = 1, \beta = 1$ and $\varphi = \pi/3$.

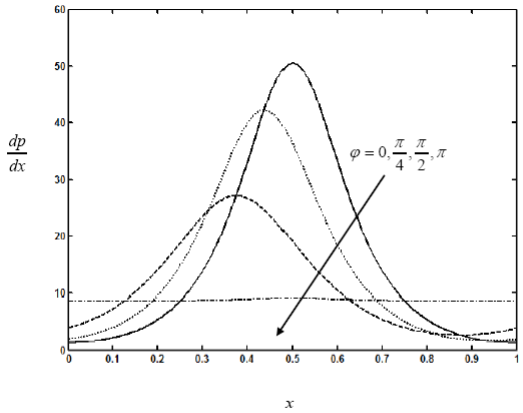

Fig. 5. The variation of axial pressure gradient $\frac{dp}{dx}$ with phase shift φ for $\phi_1 = 0.5, \phi_2 = 0.5$, $Gr = 1$, $m = 0.3, Da = 0.1, \beta = 1$ and $M = 1$.

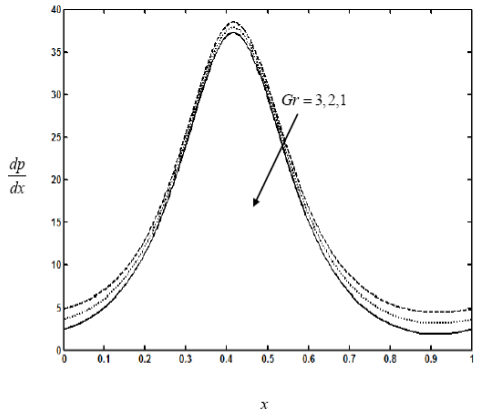

Fig. 6. The variation of axial pressure gradient $\frac{dp}{dx}$ with Grashof number Gr for $\phi_1 = 0.5, \phi_2 = 0.5,\ M = 1,\ m = 0.3, Da = 0.1, \beta = 1$ and $\varphi = \pi / 3$.

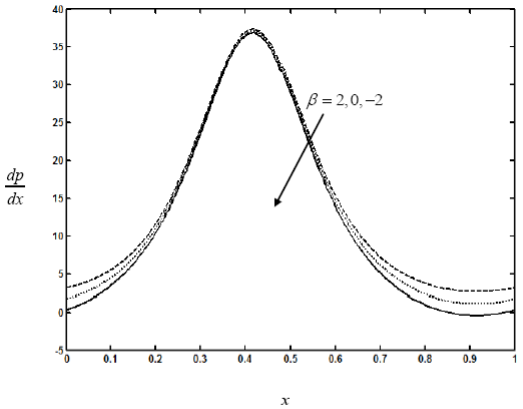

Fig. 7. The variation of axial pressure gradient $\frac{dp}{dx}$ with β for $\phi_1 = 0.5, \phi_2 = 0.5,\ Gr = 1,$ $m = 0.3, Da = 0.1, M = 1$ and $\varphi = \pi / 3$.

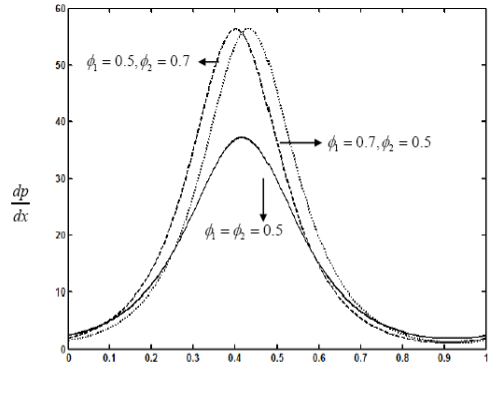

Fig. 8. The variation of axial pressure gradient $\frac{dp}{dx}$ with ϕ_1 and ϕ_2 for $\beta = 1,\ Gr = 1,$ $m = 0.3, Da = 0.1, M = 1$ and $\varphi = \pi / 3$.

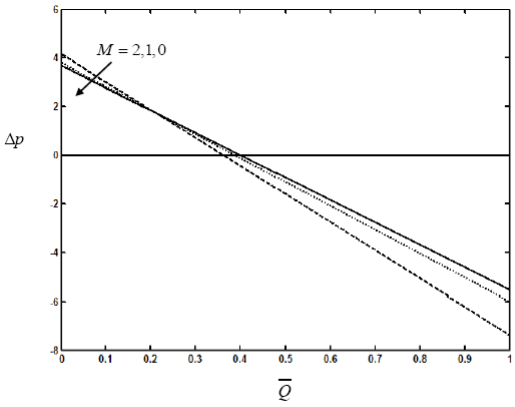

Fig. 9. The variation of pressure rise Δp with the time –averaged flux $\overline{Q}$ for different values of M with $\phi_1 = 0.5, \phi_2 = 0.5,\ Gr = 1,\ m = 0.3, Da = 0.1, \beta = 1$ and $\varphi = \pi / 3$.

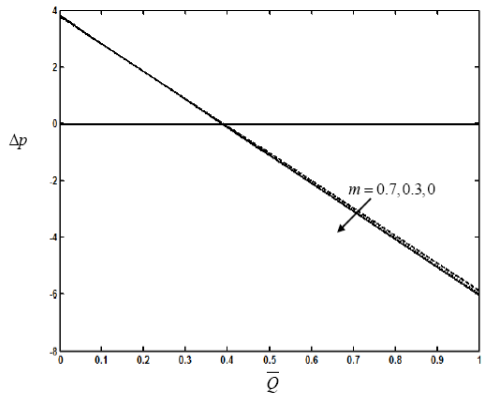

Fig. 10. The variation of pressure rise Δp with the time – averaged flux $\overline{Q}$ for different values of m with $\phi_1 = 0.5, \phi_2 = 0.5,\ Gr = 1,\ M = 1, Da = 0.1, \beta = 1$ and $\varphi = \pi / 3$.

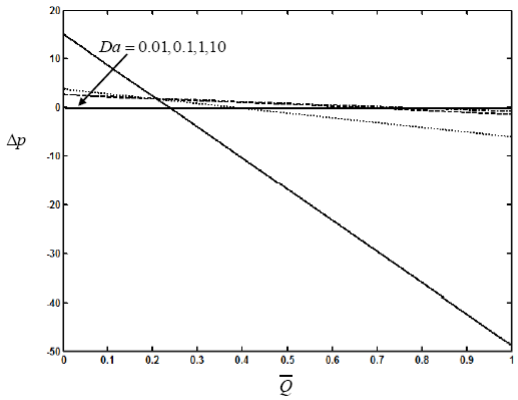

Fig. 11. The variation of pressure rise Δp with the time –averaged flux $\overline{Q}$ for different values of Da with $\phi_1 = 0.5, \phi_2 = 0.5,\ Gr = 1,\ m = 0.3, M = 1, \beta = 1$ and $\varphi = \pi / 3$.

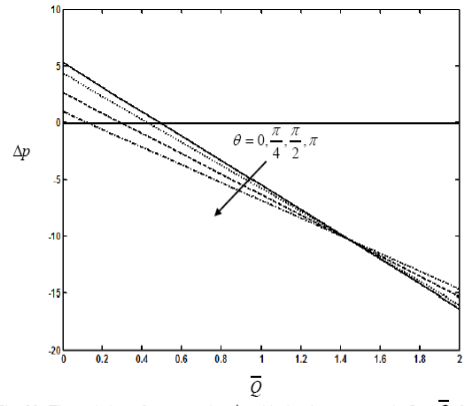

Fig. 12. The variation of pressure rise Δp with the time –averaged flux $\overline{Q}$ for different values of θ with $\phi_1 = 0.5, \phi_2 = 0.5$, $Gr = 1$, $m = 0.3, Da = 0.1, \beta = 1$ and $M = 1$.

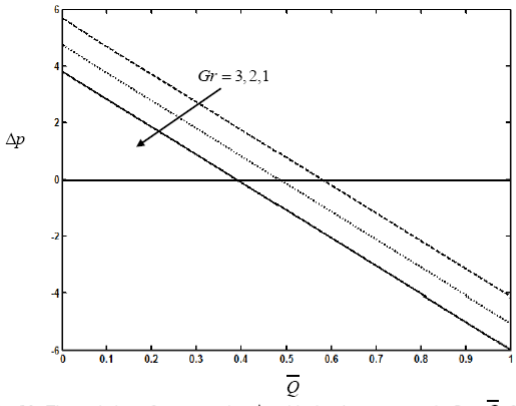

Fig. 13. The variation of pressure rise Δp with the time –averaged flux $\overline{Q}$ for different values of Gr with $\phi_1 = 0.5, \phi_2 = 0.5$, $M = 1$, $m = 0.3, Da = 0.1, \beta = 1$ and $\varphi = \pi / 3$.

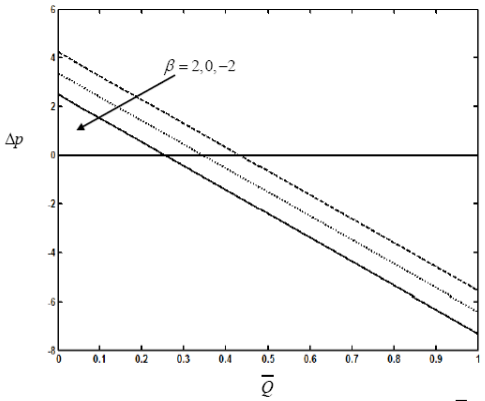

Fig. 14. The variation of pressure rise Δp with the time –averaged flux $\overline{Q}$ for different values of β with $\phi_1 = 0.5, \phi_2 = 0.5$, $Gr = 1$, $m = 0.3, Da = 0.1, M = 1$ and $\varphi = \pi / 3$.

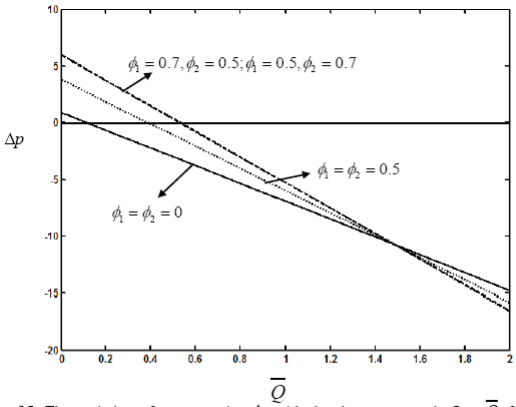

Fig. 15. The variation of pressure rise Δp with the time –averaged flux $\overline{Q}$ for different values of ϕ_1 and ϕ_2 with $M = 1$ $Gr = 1$, $m = 0.3, Da = 0.1, \beta = 1$ and $\varphi = \pi / 3$.

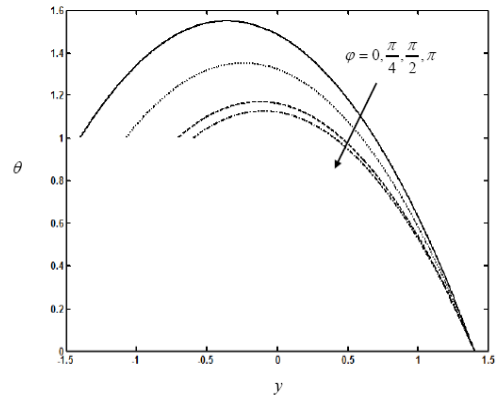

Fig. 16 The variation of temperature θ with phase shift φ for $\phi_1 = 0.5$, $\phi_2 = 0.5$ and $\beta = 1$.

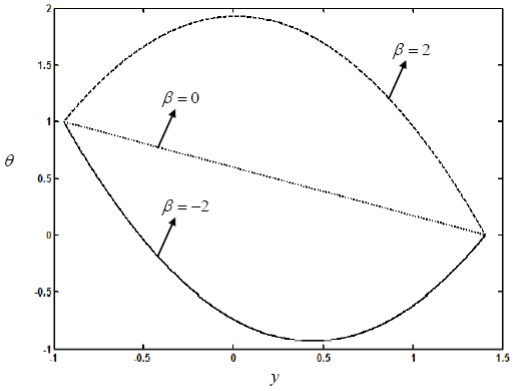

Fig. 17 The variation of temperature θ with β for $\phi_1 = 0.5$, $\phi_2 = 0.5$ and $\phi = \frac{\pi}{3}$.

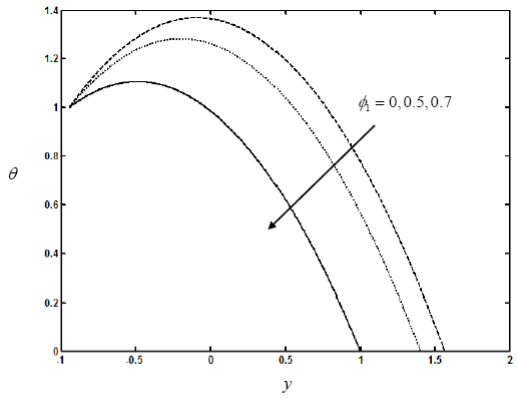

Fig. 18 The variation of temperature θ with ϕ_1 for $\varphi = \frac{\pi}{3}$, $\phi_2 = 0.5$ and $\beta = 1$.

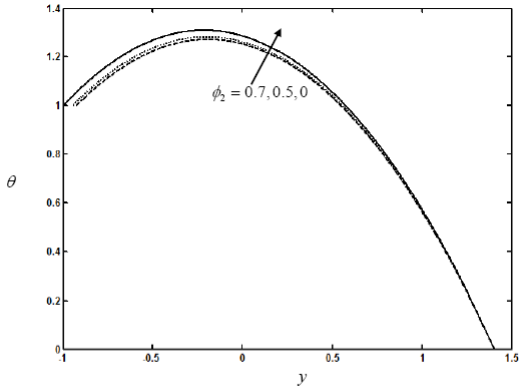

Fig. 19 The variation of temperature θ with ϕ_2 for $\phi_1 = 0.5$, $\varphi = \frac{\pi}{3}$ and $\beta = 1$.

Table 1. The variation of heat transfer coefficient Z for $x = 0.1$.

φ	β	ϕ_1	ϕ_2	Z
π/3	1	0.5	0.5	2.9568
π/2	1	0.5	0.5	2.8236
π/3	2	0.5	0.5	5.1286
π/3	1	0.7	0.5	4.2780
π/3	1	0.5	0.7	2.9446

5. CONCLUSIONS

In this paper, the peristaltic flow of a Newtonian conducting fluid through a porous medium in an asymmetric vertical channel under the effect of Hall with heat transfer is studied by using lubrication approach. The expressions for velocity, temperature and pressure gradient are obtained. It is found that, the axial pressure gradient and the time -averaged flux $\overline{Q}$ in the pumping region increases with increasing Hartmann number M, heat source/sink parameter β and free convection parameter Gr, amplitude of the upper wave ϕ_1 and lower wave ϕ_2 while the time -averaged flux $\overline{Q}$ decreases with increasing hall parameter m, Darcy number Da and phase shift φ. The heat transfer coefficient Z increases with increasing β or ϕ_1, while it decreases with increasing φ or ϕ_2.

REFERENCES

[1]. Bhatti, M. M., Ali Abbas, M. and Rashidi, M. M. Effect of hall and ion slip on peristaltic blood flow of Eyring Powell fluid in a non-uniform porous channel , World Journal of Modelling and Simulation, Vol. 12 (2016) No. 4, pp. 268-279.

[2]. El Shehawey, E.F., Mekheimer, Kh. S., Kaldas, S. F. and Afifi, N. A. S. Peristaltic transport through a porous medium, J. Biomath., 14 (1999).

[3]. El Shehawey, E.F., Sobh, A.M.F. and Elbarbary, E.M.E. Peristaltic motion of a generalized Newtonian fluid through a porous medium, . Phys. Soc. Jpn., 69(2000), 401-407.

[4]. Eldabe, N.T.M., Ahmed Y. Ghaly, A.Y., Sallam, S.N., Elagamy, K. and Younis, Y.M. Hall effect on peristaltic flow of third order fluid in a porous medium with heat and mass transfer, Journal of Applied Mathematics and Physics, 2015, 3, 1138-1150.

[5]. Eytan, O. and Elad, D. Analysis of Intra – Uterine fluid motion induced by uterine contractions, Bull. Math. Bio., 61(1999), 221-238.

[6]. Eytan, O., Jaffa, A.J. and Elad, D. Peristaltic flow in a tapered channel : application to embryo transport within the uterine cavity, Med. Engng. Phys., 23(2001), 473-482.

[7]. Govindarajan, A., Siva, E.P. and Vidhya, M. Combined effect of heat and mass transfer on MHD peristaltic transport of a couple stress fluid in a inclined asymmetric channel through a porous medium, International Journal of Pure and Applied Mathematics, Vol. 105 No. 4 (2015), 685-707

[8]. Hayat, T., Ali, N, and Asghar, S. Hall effects on peristaltic flow of a Maxwell fluid in a porous medium, Phys. Letters A, 363(2007), 397-403.

[9]. Mekheimer Kh.S. Non linear peristaltic transport through a porous medium in an inclined planar channel, J. Porous Media, 6(2003), 190-202.

[10]. Mishra, M. and Ramachandra Rao, A. Peristaltic transport of a Newtonian fluid in an asymmetric channel, Z. Angew. Math. Phys. (ZAMP), 54(2003), 532-550.

[11]. Nagendra, N., Subba Reddy, M. V. and Jayaraj, B. Peristaltic motion of a power-law fluid in an

asymmetric vertical channel, Journal of Interdisciplinary Mathematics, 11 (2008) 505-519.

[12]. Scheidegger, A. E. The physics of through porous media, McGraw-Hill, New York, 1963.

[13]. Srinivas, S. and Kothandapani, M. Peristaltic transport in an asymmetrical channel with heat transfer – A note, Int. Communications in Heat and Mass Transfer, 35(2008), 514 – 522.

[14]. Vasudev, C., Rajeswara Rao, U., Subba Reddy, M.V. and Prabhakara Rao, G. Effect of Heat transfer on peristaltic transport of a Newtonian fluid through a porous medium in an Asymmetric vertical channel, 2010, European Journal of Scientific Research, Vol. 44(1), pp. 79-92.